Gli3R-mediated inhibition of hedgehog signaling alters the embryonic transcriptome in zebrafish

Anna J. Moyer[1], Summer B. Thyme[1*]

[1] Department of Biochemistry and Molecular Biotechnology, The University of Massachusetts Chan Medical School, Worcester, MA 01605, USA

* Corresponding author

Email: Summer.Thyme@umassmed.edu

Keywords: zebrafish, embryonic development, RNA-seq, hedgehog, Gli3R, Gli, ionocytes, ion homeostasis, Foxi3, H+-ATPase-rich

ABSTRACT

Hedgehog signaling is a conserved developmental pathway that patterns diverse tissues during vertebrate embryogenesis. In zebrafish, disruptions to the hedgehog pathway cause well-characterized defects in specific cell types including neurons and glia derived from the ventral neural tube. We inhibited hedgehog signaling by overexpressing the Gli3 repressor ubiquitously and performed bulk RNA-seq of 30 hours post-fertilization zebrafish embryos. Consistent with known roles of hedgehog signaling, we observed reduced expression of genes marking lateral floor plate, motor neurons, Kolmer-Agduhr cells, dopaminergic neurons, slow muscle cells, and anterior pituitary. Gene set enrichment analysis using marker genes derived from the Daniocell atlas also revealed downregulation of genes marking H+-ATPase-rich and Na+-K+-ATPase-rich ionocytes, which are located in the embryonic skin and are responsible for osmotic homeostasis. Reduced expression of ionocyte-specific transporter genes and the transcription factor *foxi3a* suggests that Gli activity may play a previously unrecognized role in the development of this cell type.

INTRODUCTION

The hedgehog signaling pathway plays a critical role in vertebrate patterning (Ingham and McMahon 2001) and is also implicated in regeneration (Imokawa and Yoshizato 1997) and oncogenesis (Taipale et al. 2000). Depending on the context, hedgehog can act as a morphogen (Heemskerk and DiNardo 1994) or mitogen (Wechsler-Reya and Scott 1999) and specifies multiple distinct cell types across organ systems. In the canonical pathway, hedgehog ligands (Sonic, Indian, and Desert hedgehog) (Echelard et al. 1993) bind to the receptor Patched (Marigo et al. 1996; Stone et al. 1996), which relieves inhibition of the transducer Smoothened (Chen et al. 2001; Zhang et al. 2001). Activation of Smoothened shifts the balance between repressor and

activator forms of the Gli transcription factors, which in turn modulates the transcription of target genes (Ruiz i Altaba 1999; Wang et al. 2000).

Experimental manipulation of hedgehog in the zebrafish model system has revealed essential roles in development (Hammerschmidt et al. 1996; Huang and Schier 2009; Shen et al. 2013). In the presumptive spinal cord, hedgehog secreted by the notochord and medial floor plate exposes the neighboring lateral floor plate (p3), pMN, and p0-p2 progenitor domains to a gradient of hedgehog levels, which contributes to specification of neural cell types including interneurons, motor neurons, Kolmer-Agduhr cells, oligodendrocytes, and astroglia [reviewed in (Danesin and Soula 2017)]. In addition to gross morphological phenotypes like cyclopia, ventral tail curvature, and rounded somites, inhibition of hedgehog in zebrafish can expand or reduce these ventral spinal cord progenitor domains and their derivative cells (Brand et al. 1996; Chen et al. 2001; Karlstrom et al. 1996).

However, subtle differences in phenotypes result from the specific method used to disrupt hedgehog signaling (i.e., mutations, morpholinos, overexpression of Gli repressors, and chemical inhibitors). These phenotypes may vary due to compensation between paralogs, incomplete or off-target effects of antagonists, maternal contribution of mRNA in homozygous mutants, and non-canonical or hedgehog ligand-independent Gli activity. For example, knockdown of *gli1* or *gli2b* in maternal-zygotic *smoothened* mutants reduces motor neuron number compared to mutants, suggesting that basal Gli activity contributes to motoneurogenesis (Mich and Chen 2011). Similarly, overexpression of the Gli3 repressor (Gli3R) in embryos treated with the Smoothened antagonist cyclopamine reduces the number of motor neurons compared to *smoothened* mutants (England et al. 2011). These experiments highlight how changes in the expression and processing of Gli can modify specification of cells in the ventral spinal cord even in the absence of upstream hedgehog signaling.

While previous work has manipulated Gli activity in targeted phenotypic assays, the transcriptome-wide consequences of Gli3R overexpression in zebrafish remain unexplored. To address this gap, we overexpressed a zebrafish *Gli3R* (*zGli3R*) transgene (Huang and Schier 2009) ubiquitously and performed bulk RNA sequencing (RNA-seq) of 30 hours post-fertilization (hpf) zebrafish embryos. Our findings suggest that Gli activity may be involved in the development of ionocytes. We anticipate that our dataset will be most relevant to zebrafish and developmental biologists who are interested in hedgehog signaling and cell-type specification during vertebrate development.

MATERIALS & METHODS

Zebrafish husbandry and transgenesis

Animal experiments were approved by the UMass Chan Institutional Animal Care and Use Committee (IACUC protocol 202300000053). Transgenic animals were generated in an Ekkwill (EK)-based wildtype strain, and both larvae and adult animals were maintained on a 14 hour/10 hour light/dark cycle at 28°C. The *zGli3R* transgene was subcloned from *pT2-hsp-zGli3R-EGFP* into Gateway *pDONR221* (Invitrogen) and then into a Gateway-compatible *Tol2* destination vector containing the *ubb* promoter (Mosimann et al. 2011) and the *myl7:GFP* transgenesis marker. The annotated plasmid map including full sequence is available in Supplementary File 1. To produce transgenic animals using *Tol2*, one-cell embryos were injected with 1 nL of 10 ng/µL *Tol2* mRNA (Kawakami et al. 2004) and 20 ng/µL plasmid. F0 embryos with expression of the *myl7:GFP* transgenesis marker were grown to adults.

Sample collection

A mosaic F0 male was crossed to a wildtype female, and F1 embryos from one clutch were collected at 30 hpf for RNA-seq. Transgenic embryos and wildtype control siblings were sorted based on the *myl7:GFP* transgenesis marker. Four dechorionated embryos were pooled

96 and frozen on dry ice for each biological replicate, and four biological replicates were collected
97 per genotype. For live imaging, 2 days post-fertilization (dpf) and 3 dpf animals were
98 anesthetized with MS-222 and live mounted in 2% low-melt agarose (Fisher Bioreagents,
99 BP165-25) made in embryo medium with methylene blue. Images were obtained with a Leica
100 M165 FC stereo microscope and K3C color camera.

101 **RNA-seq**

102 RNA extraction, quality control, library preparation, and sequencing were conducted at
103 Azenta Life Sciences (South Plainfield, NJ, USA) as follows: Total RNA was extracted from
104 frozen tissue samples using Qiagen RNeasy Plus Universal mini kit following manufacturer's
105 instructions (Qiagen, Hilden, Germany). RNA samples were quantified using Qubit 3.0
106 Fluorometer (ThermoFisher Scientific, Waltham, MA, USA) and RNA integrity was checked
107 with 4200 TapeStation (Agilent Technologies, Palo Alto, CA, USA).

108 RNA-seq libraries were prepared using the NEBNext Ultra II RNA Library Prep Kit for
109 Illumina using manufacturer's instructions (NEB, Ipswich, MA, USA). Briefly, mRNAs were
110 initially enriched with Oligo d(T) beads. Enriched mRNAs were fragmented for 15 minutes at
111 94 °C. First strand and second strand cDNA were subsequently synthesized. cDNA fragments
112 were end repaired and adenylated at 3′ ends, and universal adapters were ligated to cDNA
113 fragments, followed by index addition and library enrichment by PCR with limited cycles. The
114 sequencing library was validated on the Agilent TapeStation (Agilent Technologies, Palo Alto,
115 CA, USA), and quantified by using Qubit 3.0 Fluorometer (Invitrogen, Carlsbad, CA) as well as
116 by quantitative PCR (KAPA Biosystems, Wilmington, MA, USA).

117 The sequencing libraries were multiplexed and clustered onto a flowcell on the Illumina
118 NovaSeq instrument according to manufacturer's instructions. The samples were sequenced
119 using a 2x150bp Paired End (PE) configuration. Image analysis and base calling were conducted

120 by the NovaSeq Control Software (NCS). Raw sequence data (.bcl files) generated from Illumina
121 NovaSeq was converted into fastq files and de-multiplexed using Illumina bcl2fastq 2.20
122 software. One mismatch was allowed for index sequence identification.

123 **RNA-seq analysis**

124 Alignment and differential gene expression analysis of RNA-seq data were performed as
125 previously described (Capps et al. 2025). Reads were aligned with the STAR aligner (2.7.3a-
126 GCC 6.4.0-2.28) (Dobin et al. 2013) to GRCz11 release 104 using the Zebrafish Transcriptome
127 Annotation version 4.3.2 (Lawson et al. 2020). Uniquely mapped reads ranged from 21.5-29.9M
128 per sample. Transcripts with zero counts in four or more of eight total samples were removed,
129 and raw counts were normalized using rlog counts in DESeq2 (Love et al. 2014). The default
130 DESeq2 method was used for determining significance, and raw and adjusted (Benjamini-
131 Hochberg) P values are in Supplementary Table 1. DESeq2 script is available on GitHub:
132 https://github.com/thymelab/BulkRNASeq.

133 Downstream analysis of bulk RNA-seq data was conducted using R (Version 4.4.2).
134 Gene set enrichment analysis (GSEA) was performed as previously described (Capps et al. 2025)
135 using the 'GSEA' function from clusterProfiler (Version 4.14.6) (Wu et al. 2021). For
136 chromosomal location GSEA, the gene set was generated using RefSeq Genes and Gene
137 Predictions from the GRCz11 assembly, and genes were sorted by abs(log2 fold change) before
138 GSEA. For Daniocell GSEA, the gene set was generated as previously described (Dang et al.
139 2025) and genes were sorted by log2 fold change before GSEA. Volcano plot, GSEA bar plot,
140 and individual gene bar plots were created using ggplot2 (Version 3.5.2) (Wickham 2016).
141 Heatmap was generated using the 'heatmap.2' function from gplots (Version 3.2.0) (Warnes et
142 al. 2025). Code to generate figures is available in Supplementary File 2.

143 **RESULTS**

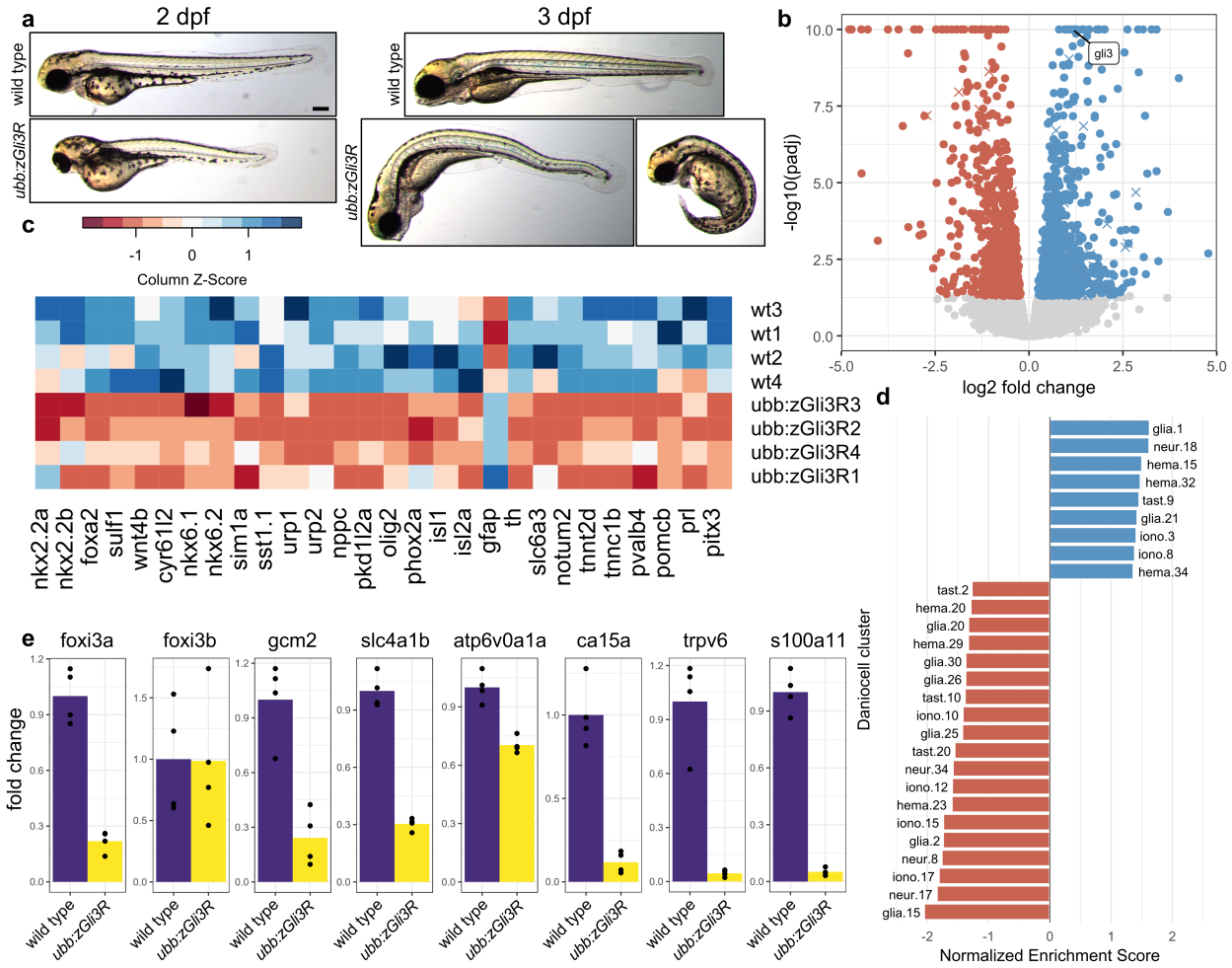

Fig. 1. Morphological and transcriptomic phenotypes of *Tg(ubb:zGli3R)* embryos. a) Representative transgenic and wildtype animals at 2 dpf and 3 dpf. Scale bar = 200 µm. b) Volcano plot comparing gene expression in 30 hpf *Tg(ubb:zGli3R)* embryos and wildtype siblings. Genes with -log10(padj) greater than ten are plotted at ten. Transcripts encoded by chromosome 4 are denoted with X symbols and transcripts encoded by all other chromosomes are denoted with circles. n=4 replicates of 4 pooled embryos for transgenic and 4 replicates of 4 pooled embryos for wildtype siblings. c) Heat map displaying expression of selected marker genes. From left to right, genes mark progenitor domains and interneurons in the ventral spinal cord, Kolmer-Agduhr cells, motor neurons, radial glia/astrocytes, dopaminergic neurons, slow muscle cells, and anterior pituitary. d) Cell types identified with GSEA using gene sets from the Daniocell single-cell atlas (Sur et al. 2023). Red bars represent terms with a negative normalized enrichment score and blue bars represent terms with a positive score. e) Bar plots of normalized counts for genes expressed in ionocytes. P values and padj for all genes are available in Supplementary Table 1.

Differential gene expression in *Tg(ubb:zGli3R)* embryos

We cloned *zGli3R* downstream of the ubiquitin B (*ubb*) promoter and co-injected F0 embryos with *Tol2* to produce transgenic lines. Transgenic F1 offspring possessed severe

163 morphological defects and died at larval stages (Fig. 1a). We isolated a mosaic F0 parent with
164 high germline transmission and performed bulk RNA-seq on 30 hpf embryos pooled from a
165 single clutch. Analysis of differentially expressed genes identified 888 upregulated genes and
166 1018 downregulated genes at a threshold of P adjusted (padj) <0.05 (Fig. 1b; Supplementary
167 Table 1). Transgene insertion can cause enrichment of differentially expressed genes based on
168 chromosomal location (White et al. 2022), and we observed a significant enrichment of genes on
169 chromosome 4 (Supplementary Table 2).

170 We next examined the expression of marker genes for cell types known to involve
171 hedgehog signaling (Fig. 1c; Supplementary Table 1). Progenitor domains in the ventral spinal
172 cord give rise to specific subtypes of neurons and glia, including interneurons, motor neurons,
173 Kolmer-Agduhr cells, oligodendrocyte precursor cells (OPCs), and astrocytes [Reviewed in
174 (Cucun et al. 2024; Danesin and Soula 2017)]. Genes marking most of these cell populations
175 were downregulated or unchanged, but *gfap*, which is expressed in radial glia and astrocyte-like
176 cells (Agius et al. 2004; Marcus and Easter 1995), was upregulated. Consistent with the
177 literature, marker genes for dopaminergic neurons (Chen et al. 2001; Holzschuh et al. 2003),
178 slow muscle cells (Blagden et al. 1997), and anterior pituitary (adenohypophysis) (Herzog et al.
179 2003) were also downregulated.

180 **Functional enrichment analysis of cell types using Daniocell single-cell atlas**

181 GSEA using gene sets derived from single-cell expression data can reveal potential
182 changes in cell composition (Capps et al. 2025; Dang et al. 2025; Moyer et al. 2025). GSEA with
183 gene sets derived from the Daniocell single-cell atlas (Sur et al. 2023) highlighted 28 clusters
184 with negative or positive enrichment compared to control (Fig. 1d; Supplementary Table 3).
185 Several of the identified clusters with negative enrichment scores, including floor plate (glia.15
186 and glia.2), Kolmer-Agduhr cells (glia.30), spinal OPCs (glia.20 and glia.26), dopaminergic

187 neurons of the diencephalon (neur.34), and anterior pituitary (tast.10) are consistent with the
188 known roles of hedgehog during zebrafish development. Other cell types with negative
189 enrichment scores included ventrolateral mesoderm (hema.20), hemangioblasts (hema.23), type
190 III taste buds (tast.2), and multiple subtypes of H+-ATPase-rich ionocytes and ionocyte
191 progenitors (iono.17, iono.15, iono.10, and iono.12). In contrast, olfactory sensory neurons
192 (tast.9), lymphoid hematopoietic stem cells (hema.15), and primitive erythroblasts (hema.32)
193 showed positive enrichment scores. Further investigation of known markers of ionocytes
194 revealed downregulation of the master regulators *foxi3a* (Hsiao et al. 2007) and *gcm2* (Esaki et
195 al. 2009; Shono et al. 2011) as well as genes expressed in H+-ATPase-rich ionocytes (*slc4a1b*,
196 *atp6v0a1a*, *ca15a*, *ceacam1*, and *si:dkey-192d15.2*), and Na+-K+-ATPase-rich ionocytes (*trpv6*
197 and *s100a11*) (Fig. 1e) (Sur et al. 2023).

198 **DISCUSSION**

199 Although activation of hedgehog signaling removes Gli3R repressor activity in some
200 contexts (Litingtung and Chiang 2000; Litingtung et al. 2002), *gli3* does not appear to be
201 expressed before 12 hpf in zebrafish (England et al. 2011; Sur et al. 2023), and activator forms of
202 Gli may possess basal levels of activity that are hedgehog ligand independent (Huang and Schier
203 2009; Karlstrom et al. 2003; Mich and Chen 2011). In this study, we explored the transcriptomic
204 consequences of overexpressing *zGli3R* ubiquitously from the earliest stages of embryonic
205 development. In contrast to experimental manipulations that inhibit hedgehog signaling, such as
206 mutations in *smoothened* or cyclopamine treatment, ectopic expression of *zGli3R* has the
207 potential to shift the balance of Gli activator and repressor forms even in the absence of
208 hedgehog signaling.

209 We first examined marker genes for cell types previously shown to depend on hedgehog
210 signaling (Fig. 1c) and then applied unbiased GSEA with Daniocell terms to discover new cell

211 types that may be regulated by Gli (Fig. 1d). The validity of our experimental approach is
212 supported by misexpression of known class II genes, which are activated by hedgehog signaling
213 and include *nkx6.1*, *nkx6.2*, and *olig2* (Fig. 1c) (Briscoe et al. 2000; England et al. 2011; Guner
214 and Karlstrom 2007). Genes marking Kolmer-Agduhr cells (*sst1.1*, *urp1*, and *urp2*), motor
215 neurons (*phox2a* and *isl2a*), dopaminergic neurons (*th* and *slc6a3*), slow muscle cells (*notum2*
216 and *tnnt2d*), and anterior pituitary (*pomcb*) were also significantly downregulated (Sur et al.
217 2023). GSEA using Daniocell gene sets identified several of the same populations, including
218 anterior pituitary (tast.10), dopaminergic neurons (neur.34), and Kolmer-Agduhr cells (glia.30).
219 However, GSEA also nominated cell types with less literature support for hedgehog involvement
220 in zebrafish, including taste buds (tast.2), hemangioblasts (hema.23), and H+-ATPase-rich
221 ionocytes (iono.17, iono.15, iono.10, and iono.12).

222 Ionocytes are specialized cells found in the embryonic skin that respond to osmotic
223 changes in the aquatic environment and are functionally analogous to amniote renal tubular cells
224 [Reviewed in (Hwang and Chou 2013)]. Progenitors derived from non-neural ectoderm give rise
225 to both ionocytes and keratinocytes (Janicke et al. 2007). Expression of the transcription factors
226 *foxi3a* and *foxi3b* in ionocyte progenitors activates Notch1 in neighboring cells, which in turn
227 suppresses ionocyte cell fate and promotes keratinocyte development (Esaki et al. 2009; Hsiao et
228 al. 2007; Janicke et al. 2007). The transcription factor *gcm2* also plays a role in the specification
229 of ionocytes (Chang et al. 2009), and we observed reduced expression of *foxi3a* and *gcm2* but
230 not of *foxi3b* (Fig. 1e).

231 Although hedgehog signaling has not been implicated in the specification of zebrafish
232 ionocytes, it does regulate *gcm2* expression during development of the amniote parathyroid
233 (Grevellec et al. 2011; Moore-Scott and Manley 2005). Moreover, the Daniocell single-cell atlas
234 shows detectable expression of hedgehog components *smo*, *ptch2*, *gli1*, *gli2a*, *gli2b*, and *gli3* in

235 non-neural ectoderm (neur.26). However, a recent study that used single-cell RNA-seq to track
236 changes in cell abundance reported that cyclopamine treatment increases the abundance of non-
237 keratinocyte epidermal progenitors and Na+-K+-ATPase-rich ionocytes (Barkan et al. 2025).
238 Future hypothesis-based approaches will determine whether *zGli3R* overexpression affects
239 ionocyte development via hedgehog signaling or by suppressing basal Gli activity.

240 **DATA AVAILABILITY STATEMENT**

241 Plasmids are available upon request. Raw RNA-seq data and gene counts have been deposited in
242 GEO (GSE307979). Processed data are available in Supplementary Table 1.

243 **ACKNOWLEDGEMENTS**

244 The authors thank Dr. Peng Huang for providing the *pT2-hsp-zGli3R-EGFP* plasmid and
245 research technician Vaishnavi Balaji for experimental support.

246 **FUNDING**

247 This work was supported by NIH grant R01 HD115159 to S.B.T. and Jérôme Lejeune
248 Foundation postdoctoral fellowship to A.J.M.

249 **LITERATURE CITED**

250 Agius E, Soukkarieh C, Danesin C, Kan P, Takebayashi H, Soula C, Cochard P. 2004. Converse
251 control of oligodendrocyte and astrocyte lineage development by sonic hedgehog in the
252 chick spinal cord. Dev Biol. 270(2):308-321.
253 Barkan E, Duran M, Lammers N, Tresenrider A, Jackson D, Lee H, Haagen B, Saunders L,
254 Abitua P, Kimelman D et al. 2025. Embryo-scale single-cell chemical transcriptomics
255 reveals dependencies between cell types and signaling pathways. bioRxiv.
256 Blagden CS, Currie PD, Ingham PW, Hughes SM. 1997. Notochord induction of zebrafish slow
257 muscle mediated by sonic hedgehog. Genes Dev. 11(17):2163-2175.
258 Brand M, Heisenberg CP, Warga RM, Pelegri F, Karlstrom RO, Beuchle D, Picker A, Jiang YJ,
259 Furutani-Seiki M, van Eeden FJ et al. 1996. Mutations affecting development of the
260 midline and general body shape during zebrafish embryogenesis. Development. 123:129-
261 142.
262 Briscoe J, Pierani A, Jessell TM, Ericson J. 2000. A homeodomain protein code specifies
263 progenitor cell identity and neuronal fate in the ventral neural tube. Cell. 101(4):435-445.
264 Capps MES, Moyer AJ, Conklin CL, Martina V, Torija-Olson EG, Klein MC, Gannaway WC,
265 Calhoun CCS, Vivian MD, Thyme SB. 2025. Disrupted diencephalon development and
266 neuropeptidergic pathways in zebrafish with autism-risk mutations. Proc Natl Acad Sci U
267 S A. 122(23):e2402557122.

268 Chang WJ, Horng JL, Yan JJ, Hsiao CD, Hwang PP. 2009. The transcription factor, glial cell
269 missing 2, is involved in differentiation and functional regulation of h+-atpase-rich cells
270 in zebrafish (danio rerio). Am J Physiol Regul Integr Comp Physiol. 296(4):R1192-1201.
271 Chen W, Burgess S, Hopkins N. 2001. Analysis of the zebrafish smoothened mutant reveals
272 conserved and divergent functions of hedgehog activity. Development. 128(12):2385-
273 2396.
274 Cucun G, Kohler M, Pfitsch S, Rastegar S. 2024. Insights into the mechanisms of neuron
275 generation and specification in the zebrafish ventral spinal cord. FEBS J. 291(4):646-662.
276 Danesin C, Soula C. 2017. Moving the shh source over time: What impact on neural cell
277 diversification in the developing spinal cord? J Dev Biol. 5(2).
278 Dang NDP, Barcus AK, Conklin CL, Truong TQ, Vivian MD, Wang J, Thomas HR, Parant JM,
279 Yeo NC, Thyme SB. 2025. Disrupted development of sensory systems and the
280 cerebellum in a zebrafish ebf3a mutant. G3 (Bethesda). 15(7).
281 Dobin A, Davis CA, Schlesinger F, Drenkow J, Zaleski C, Jha S, Batut P, Chaisson M, Gingeras
282 TR. 2013. Star: Ultrafast universal rna-seq aligner. Bioinformatics. 29(1):15-21.
283 Echelard Y, Epstein DJ, St-Jacques B, Shen L, Mohler J, McMahon JA, McMahon AP. 1993.
284 Sonic hedgehog, a member of a family of putative signaling molecules, is implicated in
285 the regulation of cns polarity. Cell. 75(7):1417-1430.
286 England S, Batista MF, Mich JK, Chen JK, Lewis KE. 2011. Roles of hedgehog pathway
287 components and retinoic acid signalling in specifying zebrafish ventral spinal cord
288 neurons. Development. 138(23):5121-5134.
289 Esaki M, Hoshijima K, Nakamura N, Munakata K, Tanaka M, Ookata K, Asakawa K,
290 Kawakami K, Wang W, Weinberg ES et al. 2009. Mechanism of development of
291 ionocytes rich in vacuolar-type h(+)-atpase in the skin of zebrafish larvae. Dev Biol.
292 329(1):116-129.
293 Grevellec A, Graham A, Tucker AS. 2011. Shh signalling restricts the expression of gcm2 and
294 controls the position of the developing parathyroids. Dev Biol. 353(2):194-205.
295 Guner B, Karlstrom RO. 2007. Cloning of zebrafish nkx6.2 and a comprehensive analysis of the
296 conserved transcriptional response to hedgehog/gli signaling in the zebrafish neural tube.
297 Gene Expr Patterns. 7(5):596-605.
298 Hammerschmidt M, Bitgood MJ, McMahon AP. 1996. Protein kinase a is a common negative
299 regulator of hedgehog signaling in the vertebrate embryo. Genes Dev. 10(6):647-658.
300 Heemskerk J, DiNardo S. 1994. Drosophila hedgehog acts as a morphogen in cellular patterning.
301 Cell. 76(3):449-460.
302 Herzog W, Zeng X, Lele Z, Sonntag C, Ting JW, Chang CY, Hammerschmidt M. 2003.
303 Adenohypophysis formation in the zebrafish and its dependence on sonic hedgehog. Dev
304 Biol. 254(1):36-49.
305 Holzschuh J, Hauptmann G, Driever W. 2003. Genetic analysis of the roles of hh, fgf8, and
306 nodal signaling during catecholaminergic system development in the zebrafish brain. J
307 Neurosci. 23(13):5507-5519.
308 Hsiao CD, You MS, Guh YJ, Ma M, Jiang YJ, Hwang PP. 2007. A positive regulatory loop
309 between foxi3a and foxi3b is essential for specification and differentiation of zebrafish
310 epidermal ionocytes. PLoS One. 2(3):e302.
311 Huang P, Schier AF. 2009. Dampened hedgehog signaling but normal wnt signaling in zebrafish
312 without cilia. Development. 136(18):3089-3098.
313 Hwang PP, Chou MY. 2013. Zebrafish as an animal model to study ion homeostasis. Pflugers
314 Arch. 465(9):1233-1247.

Imokawa Y, Yoshizato K. 1997. Expression of sonic hedgehog gene in regenerating newt limb blastemas recapitulates that in developing limb buds. Proc Natl Acad Sci U S A. 94(17):9159-9164.

Ingham PW, McMahon AP. 2001. Hedgehog signaling in animal development: Paradigms and principles. Genes Dev. 15(23):3059-3087.

Janicke M, Carney TJ, Hammerschmidt M. 2007. Foxi3 transcription factors and notch signaling control the formation of skin ionocytes from epidermal precursors of the zebrafish embryo. Dev Biol. 307(2):258-271.

Karlstrom RO, Trowe T, Klostermann S, Baier H, Brand M, Crawford AD, Grunewald B, Haffter P, Hoffmann H, Meyer SU et al. 1996. Zebrafish mutations affecting retinotectal axon pathfinding. Development. 123:427-438.

Karlstrom RO, Tyurina OV, Kawakami A, Nishioka N, Talbot WS, Sasaki H, Schier AF. 2003. Genetic analysis of zebrafish gli1 and gli2 reveals divergent requirements for gli genes in vertebrate development. Development. 130(8):1549-1564.

Lawson ND, Li R, Shin M, Grosse A, Yukselen O, Stone OA, Kucukural A, Zhu L. 2020. An improved zebrafish transcriptome annotation for sensitive and comprehensive detection of cell type-specific genes. Elife. 9.

Litingtung Y, Chiang C. 2000. Specification of ventral neuron types is mediated by an antagonistic interaction between shh and gli3. Nat Neurosci. 3(10):979-985.

Litingtung Y, Dahn RD, Li Y, Fallon JF, Chiang C. 2002. Shh and gli3 are dispensable for limb skeleton formation but regulate digit number and identity. Nature. 418(6901):979-983.

Love MI, Huber W, Anders S. 2014. Moderated estimation of fold change and dispersion for rna-seq data with deseq2. Genome Biol. 15(12):550.

Marcus RC, Easter SS, Jr. 1995. Expression of glial fibrillary acidic protein and its relation to tract formation in embryonic zebrafish (danio rerio). J Comp Neurol. 359(3):365-381.

Marigo V, Davey RA, Zuo Y, Cunningham JM, Tabin CJ. 1996. Biochemical evidence that patched is the hedgehog receptor. Nature. 384(6605):176-179.

Mich JK, Chen JK. 2011. Hedgehog and retinoic acid signaling cooperate to promote motoneurogenesis in zebrafish. Development. 138(23):5113-5119.

Moore-Scott BA, Manley NR. 2005. Differential expression of sonic hedgehog along the anterior-posterior axis regulates patterning of pharyngeal pouch endoderm and pharyngeal endoderm-derived organs. Dev Biol. 278(2):323-335.

Mosimann C, Kaufman CK, Li P, Pugach EK, Tamplin OJ, Zon LI. 2011. Ubiquitous transgene expression and cre-based recombination driven by the ubiquitin promoter in zebrafish. Development. 138(1):169-177.

Moyer AJ, Barcus A, Capps MES, Chrabasz JA, Lalonde RL, Mosimann C, Thyme SB. 2025. Genetic context of transgene insertion can influence neurodevelopment in zebrafish. bioRxiv.

Ruiz i Altaba A. 1999. Gli proteins encode context-dependent positive and negative functions: Implications for development and disease. Development. 126(14):3205-3216.

Shen MC, Ozacar AT, Osgood M, Boeras C, Pink J, Thomas J, Kohtz JD, Karlstrom R. 2013. Heat-shock-mediated conditional regulation of hedgehog/gli signaling in zebrafish. Dev Dyn. 242(5):539-549.

Shono T, Kurokawa D, Miyake T, Okabe M. 2011. Acquisition of glial cells missing 2 enhancers contributes to a diversity of ionocytes in zebrafish. PLoS One. 6(8):e23746.

Stone DM, Hynes M, Armanini M, Swanson TA, Gu Q, Johnson RL, Scott MP, Pennica D, Goddard A, Phillips H et al. 1996. The tumour-suppressor gene patched encodes a candidate receptor for sonic hedgehog. Nature. 384(6605):129-134.

Sur A, Wang Y, Capar P, Margolin G, Prochaska MK, Farrell JA. 2023. Single-cell analysis of shared signatures and transcriptional diversity during zebrafish development. Dev Cell. 58(24):3028-3047 e3012.

Taipale J, Chen JK, Cooper MK, Wang B, Mann RK, Milenkovic L, Scott MP, Beachy PA. 2000. Effects of oncogenic mutations in smoothened and patched can be reversed by cyclopamine. Nature. 406(6799):1005-1009.

Wang B, Fallon JF, Beachy PA. 2000. Hedgehog-regulated processing of gli3 produces an anterior/posterior repressor gradient in the developing vertebrate limb. Cell. 100(4):423-434.

Warnes GR, Bolker B, Bonebakker L, Gentleman R, Huber W, Liaw A, Lumley T, Maechler M, Magnusson A, Moeller S et al. 2025. Gplots: Various r programming tools for plotting data. R package version 320.

Wechsler-Reya RJ, Scott MP. 1999. Control of neuronal precursor proliferation in the cerebellum by sonic hedgehog. Neuron. 22(1):103-114.

White RJ, Mackay E, Wilson SW, Busch-Nentwich EM. 2022. Allele-specific gene expression can underlie altered transcript abundance in zebrafish mutants. Elife. 11.

Wickham H. 2016. Ggplot2: Elegant graphics for data analysis. Cham, Switzerland: Springer International Publishing.

Wu T, Hu E, Xu S, Chen M, Guo P, Dai Z, Feng T, Zhou L, Tang W, Zhan L et al. 2021. Clusterprofiler 4.0: A universal enrichment tool for interpreting omics data. Innovation (Camb). 2(3):100141.

Zhang XM, Ramalho-Santos M, McMahon AP. 2001. Smoothened mutants reveal redundant roles for shh and ihh signaling including regulation of l/r symmetry by the mouse node. Cell. 106(2):781-792.

Supplementary Materials

Gli3R-mediated inhibition of hedgehog signaling alters the embryonic transcriptome in zebrafish

Anna J. Moyer, Summer B. Thyme

Supplementary File 1: Annotated plasmid map of *pTol2-ubb:zGli3R*.

Supplementary File 2: R code to reproduce figures.

Supplementary Table 1: DESeq2 output of differentially expressed genes.

Supplementary Table 2: GSEA by chromosomal location.

Supplementary Table 3: GSEA using terms derived from Daniocell atlas single-cell data.